Journal of Himalayan Earth Sciences Volume 51, No. 1, 2018 pp. 44-60

Geo-electrical survey for the appraisal of groundwater resource in Siwalik group: a case study of Khrick Rawlakot, Azad Kashmir

Mehboob ur Rashid[1], Waqas Ahmed[*2], Sohail Anwar[1], Syed Ali Abbas[3], Sarfraz Khan[2] and Khawar Ashfaq Ahmed[4]

[1]Geoscience Advance Research Laboratory Islamabad, Geological Survey of Pakistan

[2]National Centre of Excellence in Geology, University of Peshawar

[3]Geophysics Division, Geological Survey of Pakistan Quetta

[4]Comsats Institute, Islamabad.

**Corresponding author's email: waqas.nce@gmail.com*

Submitted: 03/12/2017, Accepted: 23/03/2018, Published online: 30/03/2018

Abstract

For the groundwater resource management, the adequate knowledge and appraisal of aquifer parameters are essential. Different conventional methods are used to estimate these parameters, which are time-consuming and costly. The advent of geophysical techniques provides a cost-effective measure to estimate aquifer parameters and groundwater potential. This study attempts to model groundwater potential in Khrick, a part of Rawlakot area, Jammu and Kashmir. A hydrogeophysical survey using Vertical Electrical Sounding (VES) is adopted to outline subsurface geology and to produce a subsurface model based on the resistivity contrast of layered rocks for evaluating the groundwater accessibility. The data is acquired using Schlumberger electrode configuration, with the current electrode (AB/2) spacing 1.5 to 250 meters and potential (MN) of 1-50 meters. The VES data show that the area is composed of topsoil, shale, clayey sandstone, fractured sandstone and compact/cemented sandstone. VES at three locations (i.e. 03, 04 and 06) indicate prospects for the groundwater potential, associated with the basement complex of a sandstone bed of Siwaliks group. The true resistivity depth section maps are prepared at 40 m, 60 m, 80 m and 100 m and compared with the geoelectrical and lithological logs showing the sandstone beds as a favourable reservoir rock with true resistivity ranging between 170-400 Ωm and thickness varying from 20-100 m. The Dar-Zarrouk parameters describing the aquifer properties are also mapped, the Transverse resistance (TR) value range between 400-6200 Ωm^2, with high values, 4000-6200 Ωm^2 in the Northeastern direction. The Longitudinal conductance shows good porous beds having value in the range of 0.008-0.0128 mohos with higher values in the northwestern and southwestern directions. The aquifer thickness map prepared using the resistivity data of various lithological units revealed the northeast regions are a comparatively good potential reservoir for groundwater.

Keywords: True resistivity; Statistical Distribution; Pseudo section; Spatial model.

1. Introduction

Groundwater is essential, indispensable and unfortified natural resource, which is not efficiently being exploited since the last few decades. There is a vital need for groundwater resource estimation to build a database for effective resource estimation, land use and awareness among people. The daily intake of water by a normal healthy man is 2.5 litres/day with 200 litres/day as a domestic consumption (Hamill and Bell, 2013). According to Loague et al. (1998), more than 50% of the world's population depends on groundwater as a source of drinking, both in rural and urban areas. The ever-increasing subsisting on potable water is witnessed by population growth every year, thereby putting pressure on the public and private sector. The scarcity of safe water is further overstressed by pollutants which are channelized by groundwater to a wider area (Panagiotakis et al., 2015) According to the World Health Organization, WHO (2006) report on groundwater, contaminated and a cutoff of potable water is causing 80% of all maladies and 30 % of deaths.

To confront the stipulation of groundwater, it is extracted at an uncontrolled and alarming rate in urban, rural and domestic levels. Generally, groundwater provides the largest and easily accessible storage (Zektser and Lorne, 2004; Elizondo and Lofthouse, 2010), which possess good quality and requires little or no treatment (Asiwaju Bello et al., 2013). These uncontrolled abstractions of groundwater from boreholes are changing flow patterns and stressing the hydrogeological system. Consequently, many techniques are being adopted with the aim of hydrogeological and groundwater resource estimation. A more advanced method of resource estimation is the hydrogeophysical investigation, which adopts nonintrusive geophysical techniques, to characterize groundwater potential and drilling prospects (Arshad et al., 2007; Huang et al., 2011). Recently, the Vertical Electrical Sounding (VES) for groundwater estimation has gained popularity as it is easy to operate, allows underground structural and lithological mapping, and demarcates productive zones based on differentiating resistivity values (Martinelli, 1978; Telford et al., 1990; Maury and Balaji, 2014). It has been perceived since long that the integration of resistivity parameters extracted from surface resistivity measurement has a strong correlation between aquifer properties, as electrical properties are affected by porosity, permeability, heterogeneity, orientation of grains, compaction and consolidation (Mazac et al., 1985; Huntley, 1986; Mazac et al., 1988; Borner et al., 1996; Christensen and Sorensen, 1998; de Lima et al., 2005; Niwas et al., 2006; Rubin and Hubbard, 2006). The dependence of all these parameters governs the current flow and conduction through the soil is extremely variable and hence changes in the resistivity values (Salem, 1999).Thus, it should enter to perception from the analysis that resistivity values measured at the surface are relative in nature, not absolute and only relative correlations of hydraulic parameters are to be made. From this basic principle, surface geophysical investigations have been used since long for the subsurface delineation (Kelly 1977; Heigold et al. 1979; Huntley 1986; Frohlich et al. 1996; Salem 1999; Hubbard and Rubin 2000; Niwas and Lima 2003; Dhakate and Singh 2005; Khalil 2006; Maury and Balaji 2014).

This study is focused on the assessment and management of groundwater resources, underground lithology, and aquifer mapping by the measurement of surface electrical resistivity at Khrick, Rawlakot. So far, the groundwater resource potential of the study area has not been exploited in detail and no geophysical study has been conducted. This approach will aid to identify aquifer properties at various locations (thickness, lithology, longitudinal conductance and transverse resistance) which will provide an effective and inexpensive characterization of the aquifer and locate prime drilling locations for groundwater.

2. Study area

a. Location and physiography

The study area is a part of District Rawlakot, Azad Kashmir that lies in the Sub-Himalayan domain of the Hazara Kashmir Syntaxes (Thakur et al., 2010). The investigated area is bounded by longitudes 73° 43′ 50″ to 73° 50′00″ East and latitudes 33° 48′ 20″ to 33° 53′ 00″ North, covering parts of Survey of Pakistan toposheet No: 43 G/9. The topography of the area is uneven and is characterized by steep, rugged and undulating landscape stationed at an average elevation of 1500 m above mean sea level. The area has sub-humid to a tropical climate with average annual precipitation, 1800 mm (Nadeem, 2015). The groundwater is recharged by Rawlakot Nallah, which originates from Pir-Panjal range in the Indian part of Jammu and Kashmir.

b. Hydrogeological settings

The study area mainly consists of clastic sedimentary rocks, with three distinct lithological units: clay, shale, and sandstone present in varying proportions from shale to clayey sand, and compacted to fractured sandstone. The surficial geology is mostly comprised of Quaternary sand, shale, silt, and gravel underlain by Murree Formation of early Miocene age (Fig. 1). The Murree Formation is the oldest rock by Siwaliks group; Chinji and Nagri formations of late to middle Miocene age (Walliullah et al., 2004; Shah, 2009).

In the present work, the geological units have been categorized in the sense of aquifer characteristic (permeability, porosity, the thickness of aquifer, conductivity, and resistivity) into three hydrogeological units. The main water sources of drinking water in Rawlakot are the poor quality piped water supply, springs, and boreholes. According to the Public Health Engineering Department (PHED) of Rawlakot, there are 15,000 registered consumers with the current demand of water is about 650,000 gallons/day, whereas the existing capacity of the water plant is approximately 400,000 gallons/day.

3. Methodology

A detailed electrical resistivity technique using the vertical electrical sounding (VES) field technique is adapted to un-wrap the nature of the surface and subsurface lithologies underlying the points. The resistivity data acquisition system used in the current study is; TSQ-3 Transmitter and RDC-10 receiver of Scintrex Canada aided by the generator, stainless steel electrode, and potential electrode porous pots. The Schlumberger electrode arrangement was used for the acquisition of sounding data, to evaluate groundwater potential. The spacing arrangement for the current electrode (AB/2) going from 1.5-250 m and potential electrode (MN) from 1-50 m. Ojelabi et al. (2002) and Atakpo and Ayolabi (2009) have shown that this arrangement has a high penetration depth per unit current electrode spacing, thereby yielding maximum information of subsurface geology to a considerable depth, which is suitable for groundwater exploration. In this arrangement, four electrodes are spread along a straight line on the ground surface, and current (I) is conducted through the soil surface governed by the measurement of potential difference (ΔV) across the potential electrode. For any linear, symmetric array of AMNB electrodes, resistivity ρ can be written as equation (1):

$$\rho = k\left(\frac{\Delta V}{I}\right) \ldots\ldots\ldots\ldots\ldots\ldots\ldots (1)$$

Where ΔV is the potential difference across the potential electrodes and I is the current applied and k is the Geometric Factor and is given by equation (2).

$$k = \pi\frac{\left(\frac{AB}{2}\right)^2 - \left(\frac{MN}{2}\right)^2}{MN} \ldots\ldots\ldots\ldots\ldots\ldots\ldots (2)$$

4. Results and discussion

From the 1D-layered model generated using IPI2win resistivity software (Bobachev, 2002), the resistivity associated with each layer was derived together with corresponding thicknesses (VenkataRao et al., 2014). From the analysis, it is revealed that based on the resistivity contrast of different lithologies, the underlying strata can be categorized into three distinct lithological units of shale, clayey sand, and fractured sandstone and compact-cemented sandstone (Telford et al., 1990). The sounding curves are qualitatively and quantitatively analyzed and interpreted using inverse and forward modelling computer iteration software, IPI2win to delineate true resistivity, thickness, depth and type of

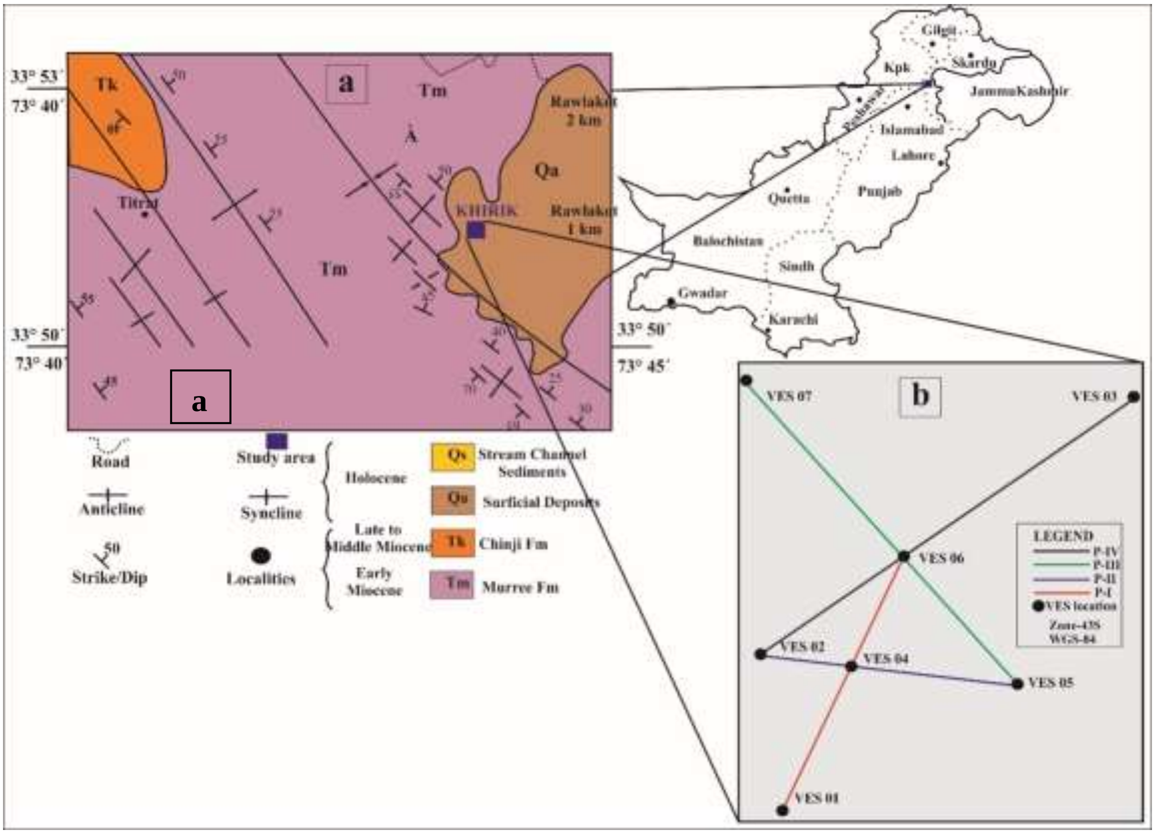

Fig. 1. a) Geological map and location of the study area modified after Walliullah et al., 2004. (b) Base Map of the study area showing VES points and Profiles I to IV.

the subsurface layers (Fig. 2). The thickness, depth and corresponding resistivity of different layers interpreted from the sounding curves are given in Table 1.

The derived resistivity curves are compared with a known resistivity of different materials to characterize the underlying lithologies (Fig. 2). Generally, the VES curve and geoelectrical sections are in agreement with the geology of the area. The resistivity of the topsoil ranges from 10-80 Ωm which is mostly saturated demarcating shaley lithological unit of the area. The second layer is characterized by clayey sandstone composition, where resistivity values fluctuate between 80-170 Ωm, with a thickness of 10-60 m. The bottom layer consists of sandstone beds and changes to a more compacted sandstone as demarcated by higher resistivity values, within a range of 170-400 Ωm. Pseudo section, resistivity cross-section, and statistical distribution curves are also prepared using iteration software to obtain a trend change in resistivity and its nature across the profile. The Spatial model of true resistivity at (AB/2) 40 m, 60 m, 80 m and 100 m depth and aquifer thickness map are also prepared, using surfer 11. Longitudinal conductance and transverse resistance of the area are also calculated by applying Dar Zarrouk Parameters (Maillet, 1947).

a. Pseudo section

Pseudo sections have been generated for seven VES, stacked along four profiles to portray the heterogeneity of resistivity with depth over the focuses considered in a profile (Fig. 3). The pseudo sections of apparent resistivity display a linear change in resistivity with depth. These pseudo sections reveal that topsoil is low resistivity

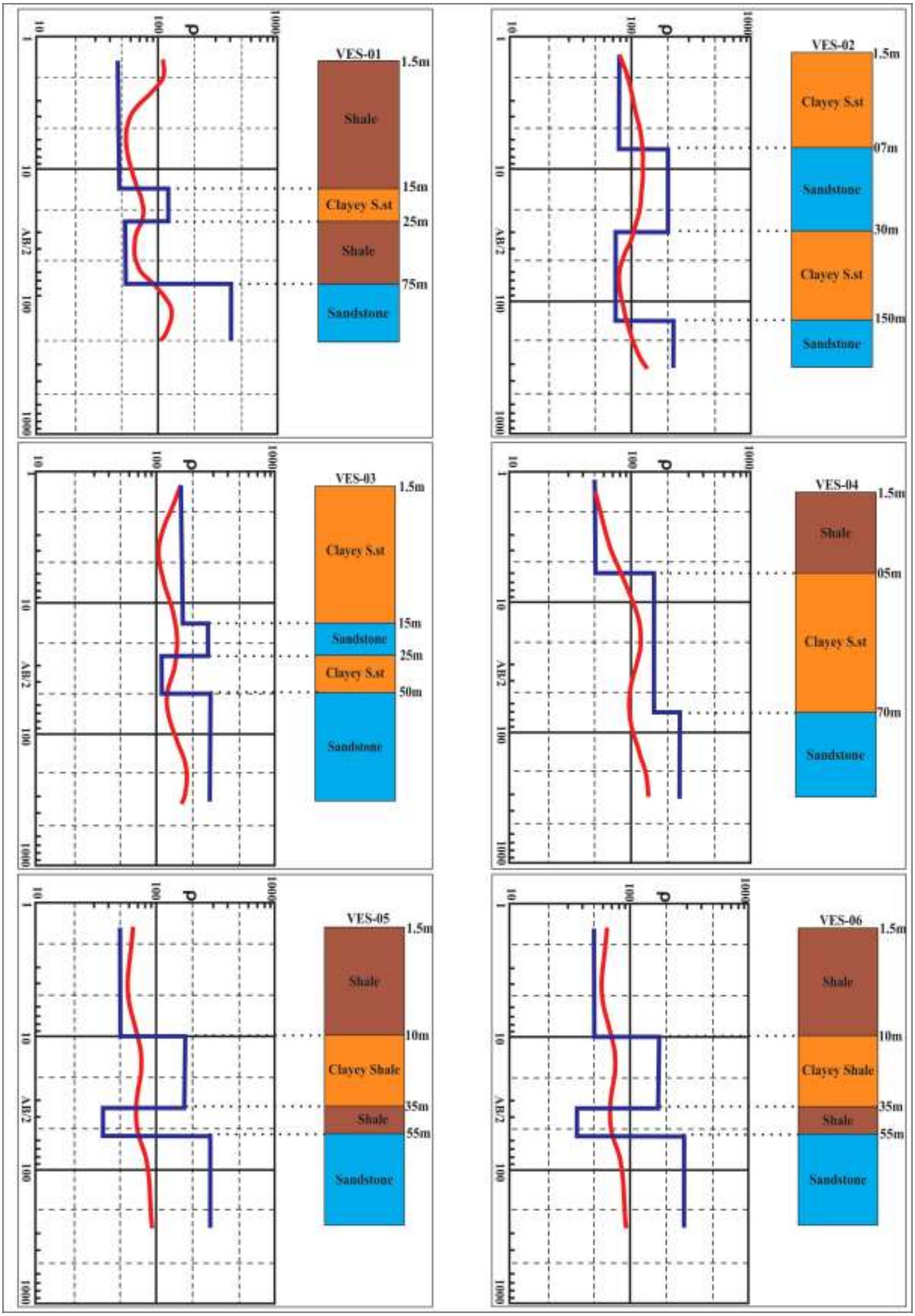
VES-01
1.5m
Shale
15m
Clayey S.st
25m
Shale
75m
Sandstone
VES-02
1.5m
Clayey S.st
07m
Sandstone
30m
Clayey S.st
150m
Sandstone
VES-03
1.5m
Clayey S.st
15m
Sandstone
25m
Clayey S.st
50m
Sandstone
VES-04
1.5m
Shale
05m
Clayey S.st
70m
Sandstone
VES-05
1.5m
Shale
10m
Clayey Shale
35m
Shale
55m
Sandstone
VES-06
1.5m
Shale
10m
Clayey Shale
35m
Shale
55m
Sandstone

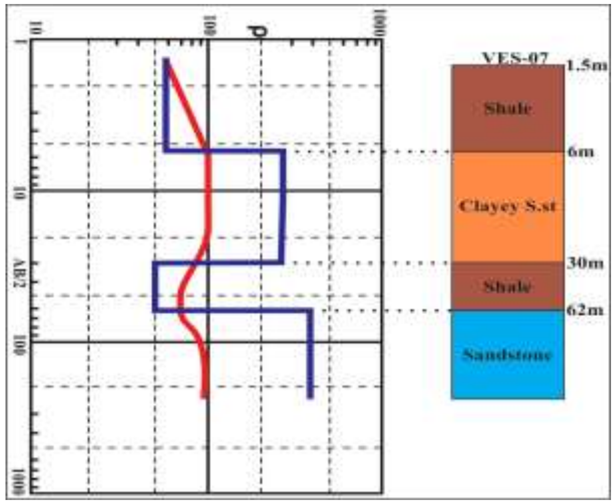

Fig. 2. Geoelectrical lithological section numerical modelled VES data of the study area using IPI2win.

Table 1. Summary of VES analysis.

VES	Layer	ρ (Ωm)	T(m)	D(m)	VES	Layer	ρ (Ωm)	T(m)	D(m)
1	WeatheredS.st	137	1.5		5	Clay	65	2	
	Shale	32	3	4		Shale	28	2	4
	FracturedS.st	174	5	9		Compact S.st	305	3	7
	Shale	23	11	20		shale	18	8	15
	CompactS.st	416	80	100		FracturedS.st	221	32	47
	Shale	20	100			Clayey shale	41	83	130
2	Clay	53	1.5	1.5		FracturedS.st	254	120	
	WeatheredS.st	142	12.5	14	6	Clayey Shale	53	3	
	Clayey sand	81	76	91		FracturedS.st	268	3	6
	CompactS.st	245	159			Shale	38	16	22
3	WeatheredS.st	176	1.5			CompactS.st	302	29	51
	Clayey Shale	42	0.5	2		Clayey Sand	106	186	237
	WeatheredS.st	130	4	6		CompactS.st	980	13	
	CompactS.st	330	6	12	7	Clayey Shale	56	1.5	
	Shale	40	17	29		FracturedS.st	270	1.5	3
	CompactS.st	890	37	66		shale	34	3	6
	Shale	26	184			FracturedS.st	284	5	11
4	Shale	50	2			Shale	25	17	28
	WeatheredS.st	174	11	13		FracturedS.st	276	40	68
	Clayey Shale	51	21	34		Clayey Shale	61	182	
	WeatheredS.st	171	216						

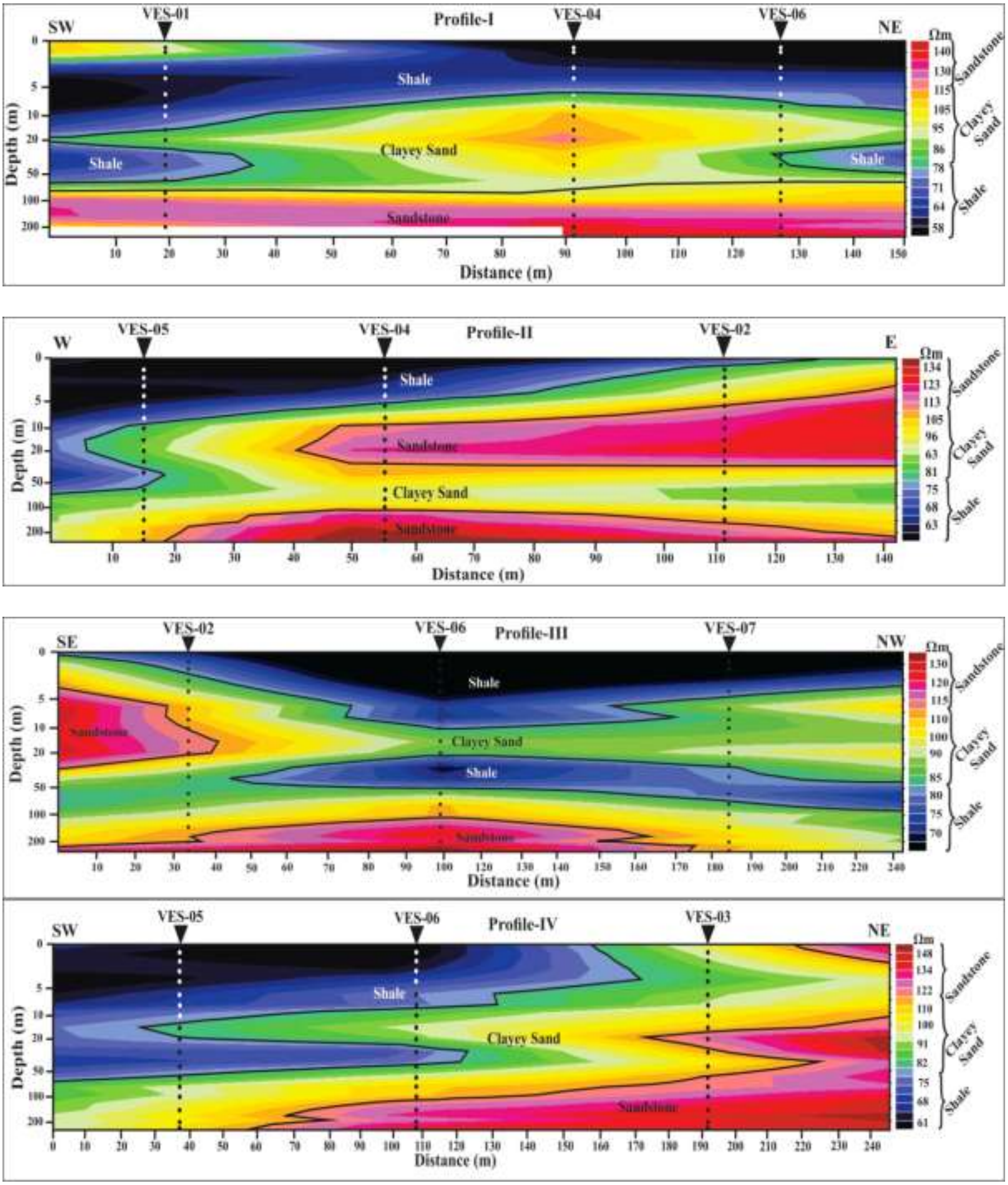

Fig. 3. Apparent resistivity Pseudo section of VES01 to VES07 stacked along P1-P4.

shale (50-80 Ωm) with a depth range of 10-20 m. The second unit encountered in all the profiles is clayey sand; the resistivity of this layer gradually increases with depth within the limits of 80-120 Ωm, and thickness of 10-200 m across profile 1. With further increase in depth, the resistivity value changes from moderate to high, i.e. between 120-150 Ωm. This high resistivity zone is marked at a depth of 50-200 m demarcated by all sounding points (VES-01 to VES-07) and inferred as sandstone beds overlain by clayey sand having good ground water potential. The pseudo sections revealed two aquifer zones, shallow confined and unconfined. As in profile-2 and profile-3, the confined aquifer is pictured by resistivity sounding as clayey sandstone bed and confined by shale on the top and bottom, making it as a sealing horizon. The non-confined aquifer, in the form of sandstone lithological unit, is present in the greater depth of 60-100 m from the surface.

From the pseudo section of the profile 3 and 4, it is deduced that sandstone beds become shallower in the northeast and southeast sides of the study area as depicted by VES-02, VES-03, and VES-04. The sections also show that the sandstone has inclined bedding, with an increase in the depth towards the northwest and southwest direction. It is inferred from the pseudo section that the recharge of the aquifer is halted by low resistivity shale beds. At more depth, the resistivity values increase uniformly, indicating hard rock aquifer in the form of sandstone lithology.

b. Resistivity section

Resistivity section is generated for the same sounding points and profiles for which the pseudo section is generated (Fig. 4). The resistivity section displayed the true picture of resistivity that changes in ascending values in a uniform manner with depth. The resistivity section of all the profiles is characterized by low resistivity top of shale with a value of 10-80 Ωm. The average thickness of the top layer is 1.5-20 m. The moderate resistivity values of 80-170 Ωm, with an average thickness of 10-60 m correspond to clayey sandstone. It is inferred from the sections that resistivity gradually increases with depth and reach to a peak value of 400 Ωm representing sandstone lithological unit at depth. The general trend of resistivity shows the presence of sandstone beds at a greater depth. The resistivity section is in agreement with the pseudo section, showing sandstone at shallow depth as displayed by Ves-02, 03 and Ves-04 along profile-02 and 03. The water reservoir of good quality and maximum recharge is mostly concentrated at a resistivity value of 120-650 Ωm showing loose, fractured and massive sandstone beds having good porosity and permeability that may prove as a reservoir-aquifer.

c. Statistical distribution curve

Statistical distribution curve (SDC) is generated by IPI2win to show mean statistical distribution of resistivity values along the profiles (1 to 4). The resistivity values for profile 01-04 to a depth of 250 m are displayed to decipher the trend of resistivity and lithological variation (Fig. 5). From SDC it is deduced that surface deposits, mostly composed of shale are up to a depth of 10 m (P-I), 6 m (P-II), 5 m (P-III) and 10 m (P-IV) and have a resistivity of 65-75 Ωm. The second zone has a lithological fabric of clayey sandstone in a depth range of 10-30 m (P-I), 6-42 m (P-II), 5-42 m (P-III) and 10-35 m (P-IV) with resistivity values of 80-120 Ωm. The third, narrow zone of a shaley composition is at a depth range of 30-45 m (P-I), 42-62 m (P-II), 42-62 m (P-III) and 35-45 m (P-IV), followed by clayey sandstone. This shaley zone is acting as a sealing horizon for clayey sandstone above, forming a confined aquifer. The fourth zone constitutes of clayey sandstone to a depth of 45-80 m (P-I), 62-148 m (P-II), 62-148 m (P-III) and 45-105 m (P-IV), underlain by sandstone at greater depth. At depth beyond 80 m (P-I), 148 m (P-II and III) and 105 m (P-IV) there is a sandstone unit with mean resistivity value of 100-150 Ωm. The general trend of SDC curve agrees with the pseudo section (Fig. 3), resistivity cross-section (Fig. 4) and geology of the area. The SDC also confirm the presence of two aquifer zones confined in the shape of clayey sandstone and unconfined aquifer of sandstone lithology.

d. Spatial model of apparent resistivity

The resistivity distributions of subsurface layers are modelled by applying Kriging interpolation techniques using Surfer-11. The Kriging interpolation technique creates smooth surfaces and incorporates anisotropies in an efficient and natural manner (Yang et

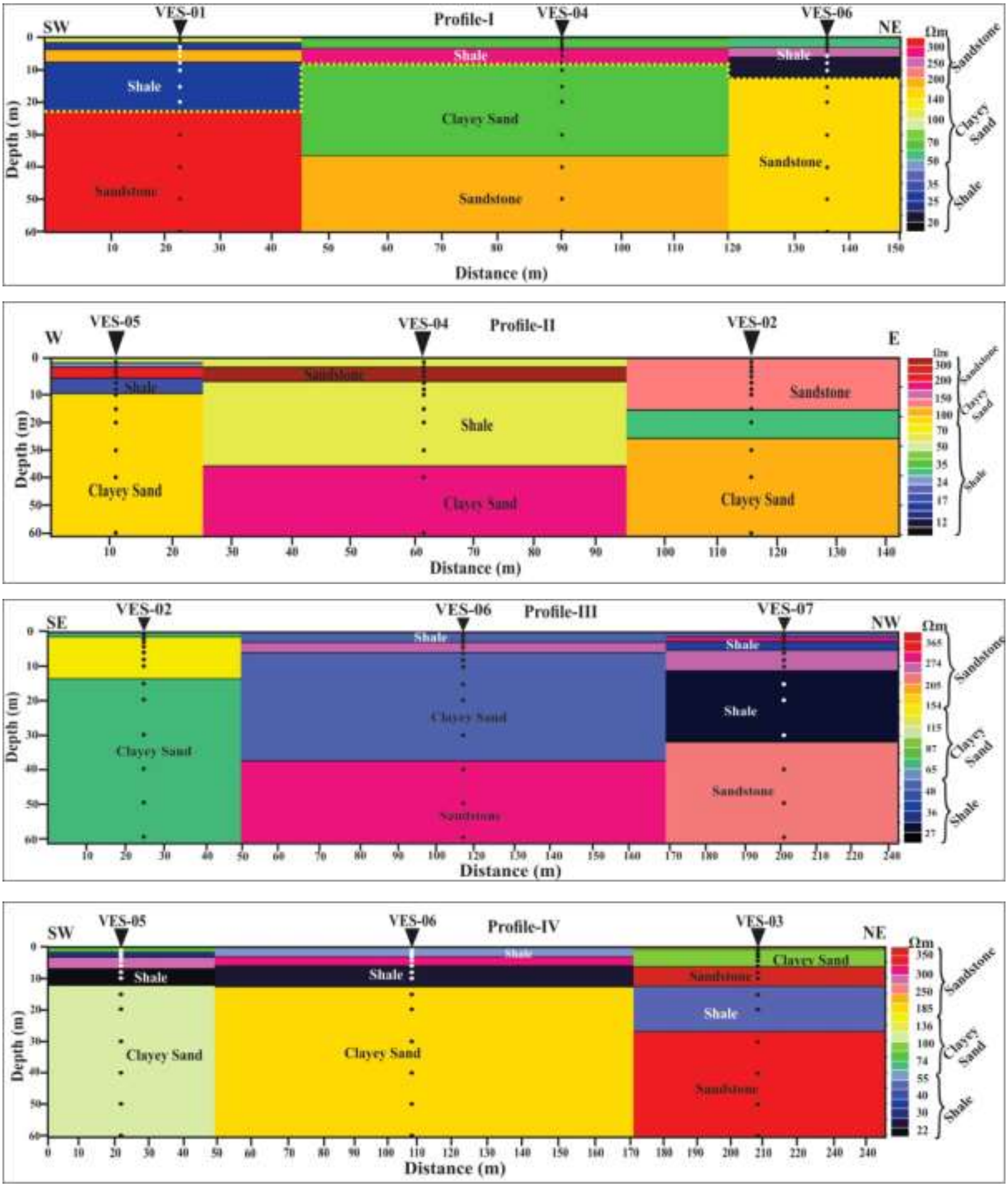

Fig. 4. Resistivity cross section of VES01 to VES07, stacked along P1-P4.

al., 2004). The spatial distributions of apparent resistivity are modelled and maps are prepared with a basic principle of changing depth (AB/2) 40 m, 60 m, 80 m and 100 m (Fig. 6).

The resistivity distribution at 40 m depth varies from 64-114 Ωm (Fig. 6a), as delineated by VES-01-07. It is perceived that the maximum resistivity value within the range ≥ 100 Ωm is observed in the northeastern and southeastern sides along VES-02, VES-03 and VES-04. In the northwest and southwest directions resistivity values drop down gradually to 64 Ωm, as observed along VES-07, VES-06, VES-05, and VES-01. It can be interpreted that the northeast and southeast sides have a thick bed of sandstone, while the northwest and southwest sides are predominantly composed of shale.

The increase in depth further to 60 m is marked by a rise in resistivity value within a limit of 66-120 Ωm. The trend of resistivity remains consistent as in Fig. 2, 3 and 4, but there is a propagation of the resistivity zone towards southwest direction. The maximum resistivity is in the northeast corner reaching to 120 Ωm, and low value in southwest corner with a value of 66 Ωm. The true resistivity section at 80 m depth shows a high to moderate resistivity at the northwest and southwest sides with values of 75-145 Ωm (Fig. 6c). It is shown by the section that the maximum resistivity value, 145 Ωm is on the northeast side and the zone becomes wider to the northwest and southwest as shown by the moderate resistivity values of 100-110 Ωm. At 100 m depth, the resistivity section shows higher values (80-160 Ωm) compared to the other sections but following the similar trend. Generally, in all the resistivity cross sections, the resistivity values increase with depth that gradually and the zone of high resistivity becomes wider and broader towards the northwest and southwest directions.

After the analysis of resistivity distribution at changing depth, it can be established that the northeast and southeast sides are dominated by a sandstone unit that gets compacted with an increase in its thickness with depth. The northwest and southwest sides are dominated by shaley lithology, deduced by the low resistivity values. The shale beds become thinners and gradually replaced by sandstone at greater depth, as confirmed by the increasing resistivity values. As shown in Figure 4, the resistivity values normally increase from the southwest to northeast in a regular manner. The northeast side of the section has sandstone beds of considerable thickness. It is inferred that the maximum clay and shale content is at 40 m depth and with a further increase it is gradually replaced by sandstone. Hence, a better reservoir may be encountered at the depth of 80-100 m but due to clay content, it is not recommended for drilling to puncture the fractured zone.

5. Characteristic of aquifer parameters

Transverse unit resistance, longitudinal unit conductance and aquifer thickness maps are produced to characterize aquifer properties. Two of the most important parameters in electrical prospecting is the longitudinal unit conductance (S) and the transverse unit resistance (TR), which define the Dar Zarrouk Parameters (DZP) (Maillet, 1947). Eq-3 and 4 define these two parameters in empirical form.

$$S=h/r \ldots\ldots\ldots\ldots\ldots \quad (3)$$

$$TR = r.h \ldots\ldots\ldots\ldots\ldots\ldots\ldots\ldots \quad (4)$$

Where h is the thickness of the lithological unit and r is its resistivity.

Transverse unit resistance describes the areas with high recharge capability and renders it the best ground exploration site of the area. Transverse unit resistance values range from 500-6200 Ωm^2 (Fig. 7). The maximum value of TR is recorded on the NE side along VES-04 and VES-06 within a limit of 4000-6200 Ωm^2. The region around VES-01, VES-05, and VES-07 is characterized by low TR with a value of 500-1000 Ωm^2, while the moderate value is recorded along Ves-02 and VES-03 in a range of 3500-4000 Ωm^2. From the analysis of TR map, it is inferred that the northeast side around VES-03 and VES-04 has a good recharge capability and extent compared to the other sides.

The longitudinal conductance (S) is the geoelectrical parameter, used to demarcate areas of groundwater potential based on unit resistivity over a known thickness. Areas

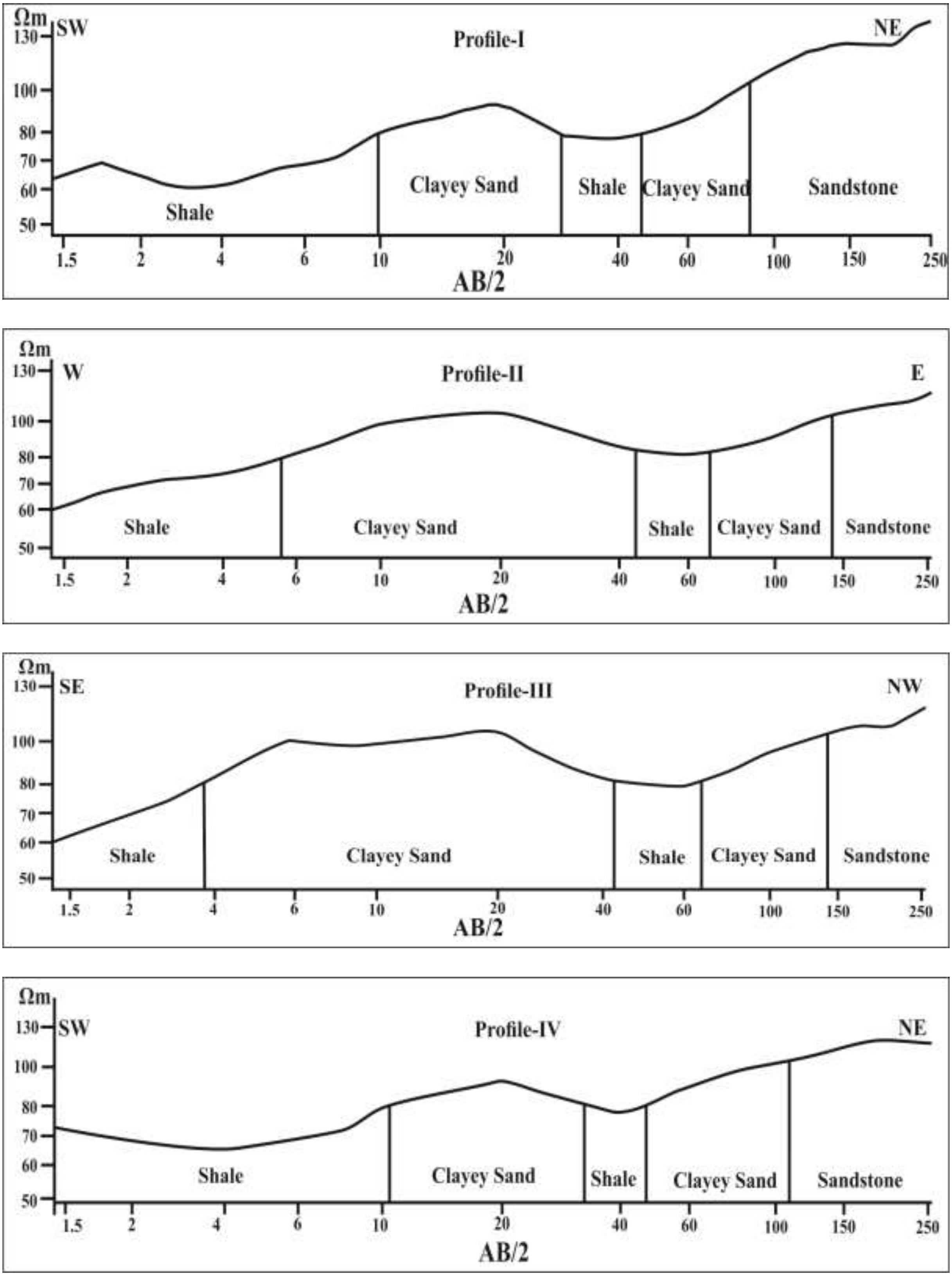

Fig. 5. Statistical Distribution curve of profile I to Profile IV.

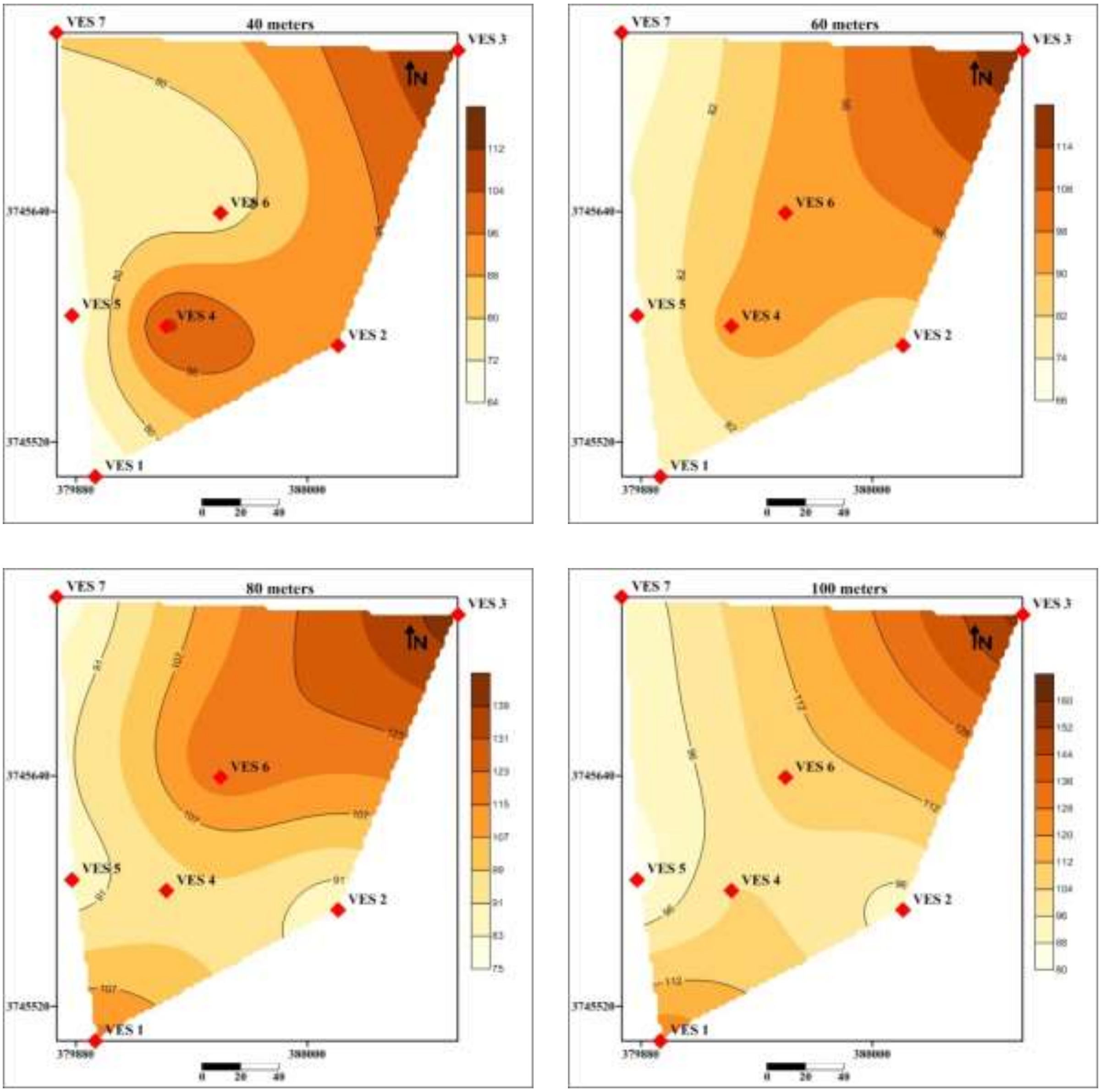

Fig. 6. Spatial distribution of apparent resistivity at (AB/2) 40 m, 60m , 80m and 100 m of the study area.

characterized by high S values normally indicate a relatively thick conductive succession of good porosity. The S of the study area varies between 0.008-0.0128 mohos (Fig. 8), high values of S (0.0108-0.0128 mohos) is observed in the northwest and southwest sides indicating shaley composition, making it conductive. Themoderate value of S (0.0094 - 0.0108 mohos) is observed around VES-04 and VES-06, while low value (0.0094-0.008 mohos) is observed around VES-02 and VES-03. This indicates that sandstone content increases toward the northeast and southeast sides of the study area. The aquifer thickness map is prepared to decipher the maximum thickness and extent of the desired recharge (Fig. 9). The thickness of the aquifer is obtained from the geoelectrical section, pseudo section and resistivity section, demarcated by VES that changes between 10-60 m, with maximum thickness around VES-04 and 06 (48-60 m) and minimum thickness around VES-01-05 and 07 (08-38 m). In general, the maximum thickness is observed on the northeast side and minimum in the southwest.

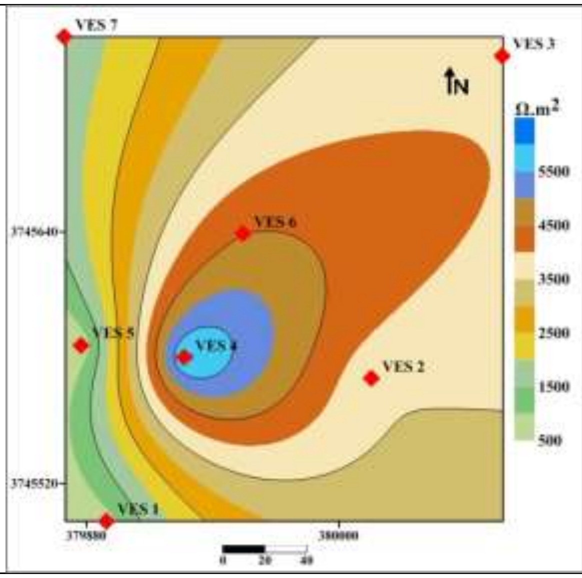

Fig. 7. Transverse resistance (TR) map for the study area

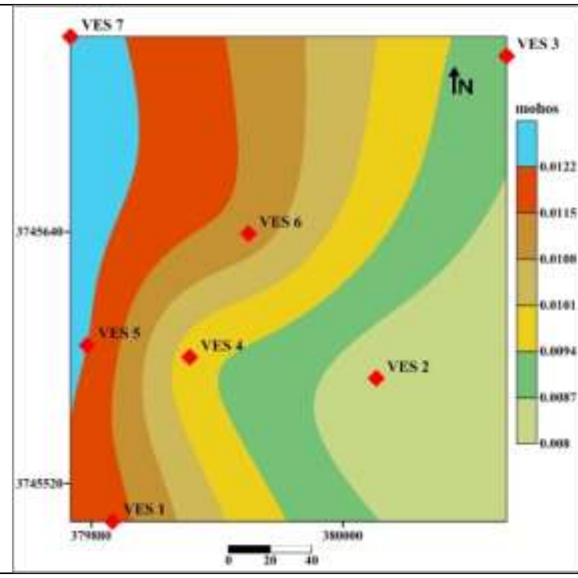

Fig. 8. Longitudinal conductance (S) map for the study area.

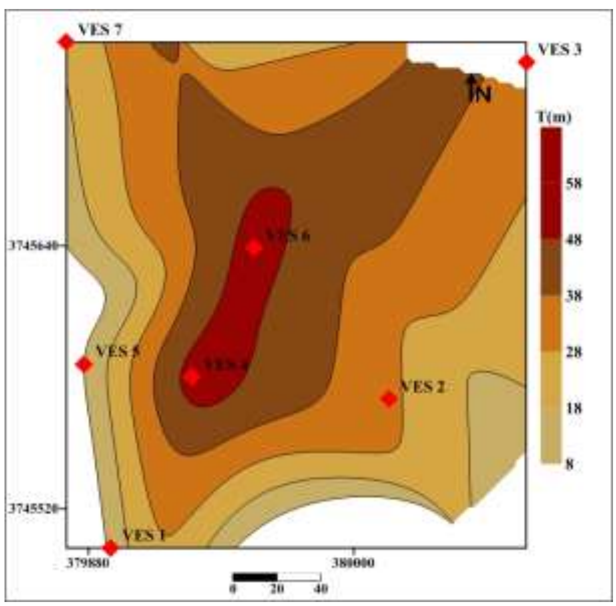

Fig. 9. Aquifer thickness map of the study area.

6. Conclusions

On the basis of VES results and prevailing knowledge about the geology of the study area, it is concluded that;

- The area is mainly composed of three basic lithological units that are; fractured to compacted and cemented sandstone, clayey sandstone, and shale beds. The two lithological units, sandstone and clayey sandstone of Nagri Formation having high and medium permeability respectively, forming the reservoir in the study area. The third, top unit is primarily composed of shale and clay with thickness range between 1.5-10 m, is formed as a result of the weathering of parent rocks, having a low permeability that halts the vertical flow of the water in recharging the aquifer.

- Shale is present as topsoil up to 10m depth having low resistivity values (10-80 Ωm) and good porosity, holding some surficial water. However, being less permeable, topsoil slows down the recharge of underground reservoirs. The second zone is clayey sandstone having higher resistivity values (80-170 Ωm) with a thickness range of 10-50 m, forming confined aquifer of the area.
- The transverse resistance increases in the Northeastern (NE) direction, with a maximum value of 4000-6200 Ωm^2 around VES-04 & 06, showing sandstone beds with maximum recharge capacity. The Longitudinal conductance increases in the Northwestern (NW) and southwestern (SW) direction showing shaley beds with maximum porosity. The Dar-Zarrouk parameters indicate sandstone beds on the NE side with good water potential and shaley beds in the NW-SW side with poor recharge capability. The thickness of aquifer beds increases in the Northeastern side with a maximum thickness of 60 meters.
- Porous and fractured sandstone is the main zone for the water accumulation and is regarded as productive, inferred from the true resistivity value of 170-400Ωm. The area is divided into two zones; the northeast and southeast side, dominated by shallow sandstone unit, and the northwest and southwest side, dominated by shaley lithology near the surface.
- The northwest and southwest zone reflects the fractured sandstone, with intercalation of shale and clay. This zone has the least capacity to retain water and the surface recharge is halted by shaley lithology, therefore, it may not prove a good groundwater aquifer and should not be targeted for the conformity bore drilling. Whereas, the presence of a thick unit of sandstone beds at the northeast and southeast side's show a good groundwater potential. The transverse resistance and aquifer thickness also increase towards the northeast side of the study area, with a maximum thickness recorded around Ves-04 and 06.
- The lateral extent of the aquifer and recharge will remain the main consideration, even if the productivity at the particular site is proven. It is therefore recommended to carry out long profiles, to study deep zones for prospect generation, and in case of positive signs for the saturated porous zone, deep drilling up to 100 m should be carried out to puncture the entire fractured sandstone zone for larger recharge and permeability.

Acknowledgement

The authors are thankful to Dr. Imran Ahmad Khan, Ex-Director General Geological Survey of Pakistan, and the Ministry of Petroleum and Natural Resources for providing financial assistance to carry out this research project. Thanks are also due to Mr. Zahid Sarfraz, Geophysical Assistant for helping in collecting the field data, the Geophysics Division, Geological Survey of Pakistan Quetta for their valuable suggestions and support to carry out this research work and to the local community of Azad Kashmir for facilitating us during the field.

Conflict of Interest statement

On behalf of all authors, the corresponding author states that there is no conflict of interest.

Authors' Contribution

Mehboob ur Rashid, Conducted field survey, data analysis and manuscript writing.

Waqas Ahmed did data interpretation and manuscript writing and also is the corresponding author. Sohail Anwar and Syed Ali Abbas conducted field survey. Sarfraz Khan was involved in manuscript writing. Khawar Ashfaq Ahmed did manuscript writing.

References

Arshad, M., Cheema, J., Ahmed, S., 2007. Determination of lithology and groundwater quality using electrical resistivity survey. International Journal of Agriculture and Biology, 9, (1), 143-146.

Asiwaju Bello, Y. A., Olabode, F. O., Duvbiama, O. A., Iyamu, J. O., Adeyemo, A. A., Onigbinde, M. T., Arshad, M., Cheema, J., Ahmed, S., 2007. Determination of lithology and groundwater quality using electrical resistivity survey. International Journal of Agriculture and Biology, 9, (1), 143-146.

Atakpo, E. A., Ayolabi, E. A., 2009. Evaluation of aquifer vulnerability and the protective capacity in some oil producing communities of western Niger Delta. The Environmentalist, 29, (3), 310-317.

Bobachev, C., 2002. IPI2Win: A windows software for an automatic interpretation of resistivity sounding data Type. Thesis, Moscow State University, Moscow, Russia.

Borner, F., Schopper, J., Weller, A., 1996. Evaluation of transport and storage properties in the soil and groundwater zone from induced polarization measurements. Geophysical Prospecting, 44, (4), 583-601.

Christensen, N. B., Sorensen, K. I., 1998. Surface and borehole electric and electromagnetic methods for hydrogeological investigations. European Journal of Environmental and Engineering Geophysics, 3, 75-90.

De Lima, O. A., Clennell, M. B., Nery, G. G., Niwas, S. A., 2005. Volumetric approach for the resistivity response of freshwater shaly sandstones. Geophysics, 70, (1), F1-F10.

Dhakate, R., Singh, V., 2005. Estimation of hydraulic parameters from surface geophysical methods, Kaliapani Ultramafic Complex, Orissa, India. Journal of Environmental Hydrology, 13.

Elizondo, G. M., Lofthouse, V., 2010. Towards a sustainable use of water at home: understanding how much, where and why? Journal of Sustainable Development, 3, (1), 3.

Frohlich, R. K., Fisher, J. J., Summerly, E., 1996. Electric-hydraulic conductivity correlation in fractured crystalline bedrock: Central Landfill, Rhode Island, USA. Journal of Applied Geophysics, 35, (4), 249-259.

Hamill, L., Bell, F. G., 2013. Groundwater resource development. Elsevier.

Heigold, P. C., Gilkeson, R. H., Cartwright, K., Reed, P. C., 1979. Aquifer transmissivity from surficial electrical methods. Groundwater, 17, (4), 338-345.

Huang, Y. P., Kung, W. J., Lee, C. H., 2011. Estimating aquifer transmissivity in a basin based on stream hydrograph records using an analytical approach. Environmental Earth Sciences, 63, (3), 461-468.

Hubbard, S. S., Rubin, Y., 2000. Hydrogeological parameter estimation using geophysical data: a review of selected techniques. Journal of Contaminant Hydrology, 45, (1), 3-34.

Huntley, D., 1986. Relations between permeability and electrical resistivity in granular aquifers. Groundwater, 24, (4), 466-474.

Kelly, W. E., 1977. Geoelectric sounding for estimating aquifer hydraulic conductivity. Groundwater, 15, (6), 420-425.

Khalil, M. H., 2006. Geoelectric resistivity sounding for delineating salt water intrusion in the Abu Zenima area, west Sinai, Egypt. Journal of Geophysics and Engineering, 3, (3), 243.

Loague, K., Abrams, R. H., Davis, S. N., Nguyen, A., Stewart, I. T., 1998. A case study simulation of DBCP groundwater contamination in Fresno County California & transport in the saturated subsurface. Journal of Contaminant Hydrology, 29 (2), 137-163.

Maillet, R., 1947. The fundamental equations of electrical prospecting. Geophysics, 12 (4), 529-556.

Martinelli, E., 1978. Groundwater exploration by geoelectrical methods in Southern Africa. Bulletin of Engineering Geology, 15 (1), 113-124.

Maury, S., Balaji, S., 2014. Geoelectrical method in the investigation of groundwater resource and related issues in Ophiolite and Flysch formations of Port Blair, Andaman Island, India. Environmental Earth Sciences, 71 (1), 183-199.

Mazac, O., Cislerova, M., Vogel, T., 1988. Application of geophysical methods in describing spatial variability of saturated hydraulic conductivity in the zone of aeration. Journal of Hydrology 103, (1-2), 117-126.

Mazac, O., Kelly, W., Landa, I. A., 1985. hydrogeophysical model for relations between electrical and hydraulic properties of aquifers. Journal of Hydrology, 79, (1-2), 1-19.

Nadeem, F., 2015. Pakistan Monsoon 2015 Rainfall. CDPC Technical Report, 4.

Niwas, S., Gupta, P. K., de Lima, O. A., 2006. Nonlinear electrical response of saturated shaley sand reservoir and its asymptotic approximations. Geophysics 71, (3), G129-G133.

Niwas, S., Lima, O. A., 2003. Aquifer parameter estimation from surface resistivity data. Groundwater, 41, (1), 94-99.

Ojelabi, E., Badmus, B., Salau, A., 2002. Comparative analysis of Wenner and Schlumberger Methods of Geoelectric Sounding in subsurface Delineation and groundwater exploration-A case study. Geological Society of India, 60, (6), 623-628.

Organization, W. H., 2006. Protecting Ground Water for Health-Managing the Quality of Drinking-water Sources: World Health Organization.

Panagiotakis, I., Dermatas, D., Vatseris, C., Chrysochoou, M., Papassiopi, N., Xenidis, A., Vaxevanidou, K., 2015. Forensic investigation of a chromium (VI) groundwater plume in Thiva, Greece. Journal of hazardous materials, 281, 27-34.

Rubin, Y., Hubbard, S. S., 2006. Hydrogeophysics: Springer Science & Business Media, 50.

Salem, H. S., 1999. Determination of fluid transmissivity and electric transverse resistance for shallow aquifers and deep reservoirs from surface and well-log electric measurements. Hydrology and Earth System Sciences, 3, (3), 421-427.

Shah, S. M. I., 2009. Stratigraphy of Pakistan, Geological Survey of Pakistan Publication Directorate, Quetta Pakistan, 22, 381.

Telford, W. M., Geldart, L. P., Sheriff, R. E., 1990. Applied geophysics, Cambridge University Press, Cambridge, UK.

Thakur, V., Jayangondaperumal, R., Malik, M., 2010. Redefining Medlicott–Wadia's main boundary fault from Jhelum to Yamuna: An active fault strand of the main boundary thrust in northwest Himalaya. Tectonophysics, 489, (1), 29-42.

VenkataRao, G., Kalpana, P., Rao, R. S., 2014. Groundwater investigation using geophysical methods-a case study of Pydibhimavaram Industrial area. International Journal of Research in Engineering and Technology 3, 13-17.

Nasir, S., Hussain, A., Akhtar, S. S., 2004. Geological map of Thorar Area District Rawlakot AJK and part of Rawalpindi District Pakistan 43G/9. Geological Survey of Pakistan Publication Directorate Quetta, 19, 1-1.

Yang, C. S., Kao, S. P., Lee, F. B., Hung, P. S., 2004. In Twelve different interpolation methods: A case study of Surfer 8.0, Proceedings of the XXth ISPRS Congress, 2004, 778-785.

Zektser, I. S., Lorne, E., 2004. Groundwater Resources of the World and their Use. 6th ed., Unesco place de Fontenoy Paris: France, 342.